Journal of Precision Instrument and Machinery (2024)
Clausius Scientific Press, Canada

DOI: 10.23977/jpim.2024.040104
ISSN 2616-1990 Vol. 4 Num. 1

Research on Water-Assisted Femtosecond Laser Drilling Process for Superalloy

Liang Wang[1,a], Rong Guan[2,b,*], Lei Zhao[3,c], Qunyong Zhang[4,d], Yuan Li[1,a], Changjian Wu[1,a]

[1]*Faculty of Mechanical and Material Engineering, Huaiyin Institute of Technology, Huai'an, China*
[2]*School of Art and Design, Huaiyin Institute of Technology, Huai'an, China*
[3]*Faculty of Foreign Languages, Huaiyin Institute of Technology, Huai'an, China*
[4]*Faculty of Mathematics and Physics, Huaiyin Institute of Technology, Huai'an, China*
[a]*wangliang@hyit.edu.cn,* [b]*lovemyself1103@163.com,* [c]*66264960@qq.com,*
[d]*zhangqunyong@126.com*
[*]*Corresponding author*

Keywords: Femtosecond Laser, High-Temperature Alloys, Water-Assisted, Laser Drilling, Process Optimization

Abstract: Due to its ultrashort pulse duration and extremely high power density, femtosecond laser enables "cold" material processing, offering unparalleled advantages over traditional laser processing methods. As a result, it holds great potential in fields such as high-end equipment manufacturing and ultraprecision machining. However, current femtosecond laser processing technology faces challenges such as blind selection of processing parameters and unstable processing quality, which limit its further development and application. This paper primarily analyzes the characteristics of laser micromachining, studies the interaction mechanisms between femtosecond lasers and materials, and further investigates the theoretical basis of water-assisted laser processing technology. Based on the theoretical study, GH4169 superalloy was selected as the experimental material, and a circular cutting method was adopted in a water-assisted laser processing setup. A single-factor experimental study was conducted on femtosecond laser processing of blind holes in GH4169 superalloy to explore the effects of different laser parameters on the quality of blind hole machining. The study revealed the influence patterns of scanning speed and laser pulse energy on the diameter and morphology of blind holes. Finally, by comparing and analyzing the taper and inner wall machining quality of the blind holes, the optimal processing parameters for femtosecond laser machining of blind holes in GH4169 superalloy were determined. The results verified the advantages of femtosecond laser processing in a water-based environment compared to an air environment for machining micro holes in superalloys, providing a theoretical foundation and reference for further research on water-assisted femtosecond laser processing of blind holes in superalloy.

1. Introduction

The rapid development of the economy and technology has significantly advanced China's aviation engine industry. To enhance the thermal efficiency of aviation engines by better heating compressed

air and increasing their thrust-to-weight ratio, raising the turbine inlet temperature of aviation engines has become an urgent requirement [1]. The turbine blade's ability to withstand high temperatures determines the turbine inlet temperature, which is also influenced by the cooling structures of the blades. Cooling micro holes are a crucial part of the cooling structures for turbine blades. Film cooling holes, which can be categorized into shaped holes and cylindrical holes, are typically inclined at an angle to the blade surface. Modern turbine blades often feature hundreds of cooling micro holes with diameters smaller than 0.3 mm [2]. At present, the precision machining of film cooling micro holes is a key technology for improving the temperature resistance of turbine blades in aviation engines. Compared with traditional film cooling hole machining methods, laser drilling has become a major research focus due to its higher precision and efficiency in producing cooling micro holes. Femtosecond pulsed laser processing, which can create high-quality film cooling micro holes in nickel-based superalloy turbine blades, and water-assisted laser processing, which improves micro hole quality, have been increasingly applied in practice. According to the definition of micro hole dimensions provided by domestic and international researchers, holes with diameters ranging from 0.3 mm to 1 mm are classified as small holes, while those with diameters smaller than 0.3 mm are referred to as micro holes [3]. Based on this definition, the film cooling holes in turbine blades fall under the category of micro holes.

This study conducts theoretical and experimental research on femtosecond laser processing of GH4169 superalloy. It systematically analyzes water-assisted laser processing technology and, based on theoretical insights, designs experiments for water-assisted femtosecond laser ablation of GH4169 superalloy. The aim is to provide theoretical and experimental foundations for the machining of film cooling holes in turbine blades. Using a single-factor experimental design and femtosecond laser equipment, the study investigates the effects of different laser parameters (such as pulse energy and scanning speed) on micro hole machining in different environments. Based on these investigations, process parameter optimization is carried out to determine the optimal processing parameters for femtosecond laser machining of micro holes in GH4169 nickel-based superalloy.

2. Materials and Experiment

2.1. Materials and Samples

GH4169, also known as Inconel 718, is a precipitation-strengthened nickel-based superalloy that exhibits excellent overall performance within a temperature range of -253 ℃ to 700 ℃. Below 650 ℃, its yield strength ranks highest among deformation superalloys [4]. GH4169 offers high heat resistance, excellent fatigue performance, superior high-temperature oxidation and corrosion resistance, and long-term structural stability in high-temperature environments, making it suitable for manufacturing complex components. Due to its outstanding properties, GH4169 superalloy is widely used in producing hot-end components of aviation turbine engines and various high-temperature load-bearing structural components in aerospace rocket engines [5]. Additionally, GH4169 is extensively applied in other fields such as energy (e.g., nuclear reactor components and high-temperature gas furnace heat exchangers) and automotive manufacturing (e.g., gas turbines and automotive turbochargers). With the advancement of modern industries, the demand for machining GH4169 superalloy continues to grow. Against this backdrop, GH4169 superalloy was chosen as the experimental material for the femtosecond laser drilling experiments due to its high research value. The chemical composition and content of GH4169 superalloy are detailed in Table 1.

Table 1: Chemical composition and component proportion of GH4169[6]

Alloy Grade	Chemical Composition and Content /%							
GH4169	C	Cr	B	Ni	Co	AI	Ti	Nb
	0.025	19.51	0.001	53.5	0.2	0.5	0.85	5.00
	Si	S	Mo	Mn	P	Cu	B	Fe
	0.02	0.01	2.97	0.05	0.002	0.05	0.0002	margin

2.2. Material Preparation

To meet the experimental machining requirements and ensure compatibility with measurement equipment, it is essential to prepare the experimental materials properly. Before the experiment, the purchased GH4169 superalloy rods were processed using a CNC electrical discharge wire-cutting machine to create cylindrical raw materials with a base radius of R=15 mm and a thickness of D=3 mm. The front and back surfaces of the experimental materials were then subjected to rough grinding using sandpaper of models 180Cw and 400Cw. Subsequently, precision grinding was performed using 2000Cw sandpaper to achieve a smooth surface finish on the GH4169 superalloy[7]. After grinding, the GH4169 superalloy samples were thoroughly cleaned multiple times with anhydrous ethanol. Once the samples were air-dried, they were placed in sealed sample bags for storage, with appropriate material labeling. This completed the material preparation process.

2.3. Experimental Method

Based on theoretical analysis, this experiment uses a single-factor experimental method to study the effects of various variables on the quality of femtosecond laser drilling of GH4169 superalloy micro holes under different processing environments. Specifically, pulse energy and scanning speed are selected as the single-factor experimental variables for comparison experiments of femtosecond laser processing on the superalloy in different environments.

Nitrogen gas is chosen as the auxiliary gas, with coaxial gas blowing as the auxiliary method (where the direction of the auxiliary gas flow is the same as the direction of the laser beam during the machining process). The use of auxiliary gas helps protect the focusing lens, preventing molten material and debris generated during the femtosecond laser processing of the superalloy micro holes from contaminating the lens[8]. Additionally, because the blow-off function of the femtosecond laser processing equipment cannot be manually turned off during the experiment, to avoid experimental errors caused by the auxiliary gas blowing away the water medium from the material surface during the water-assisted laser processing comparison experiments, a transparent glass sheet is placed between the femtosecond laser nozzle and the water-based medium in the actual experiments[9]. (see Table 2)

Table 2: Single-Factor Experimental Design

No.	Single Pulse Energy (μJ)	Scanning Speed (mm/min)	Processing Environment	Pulse Width (fs)	Spot Diameter (μm)	Repetition Frequency (kHz)	Scan Count (times)
I	20-140	400	air	276	36	50	40
II	20-140	400	water	276	36	50	40
III	140	50-800	air	276	36	50	40
IV	140	50-800	water	276	36	50	40

3. Results and Discussion

3.1. Impact of Single Pulse Energy on Erosion Hole Quality

Laser pulse energy refers to the energy carried by the laser in a single pulse cycle[10]. In practical micro hole manufacturing, pulse energy plays a critical role in the machining efficiency and the maximum drilling depth of small holes. As the pulse energy increases, both the micro hole machining efficiency and the maximum drilling depth also increase. However, with the continuous increase in laser energy, the thermal effects generated during the micro hole processing also become more pronounced, leading to a decrease in the quality of the micro hole.

From the experimental results shown in Figure 1, Figure 2 and the trend chart in Figure 3, it can be observed that in both processing environments, as the single pulse energy of the femtosecond laser increases, the obtained blind hole entrance diameter, depth, and depth-to-diameter ratio significantly increase, while the blind hole taper decreases significantly.

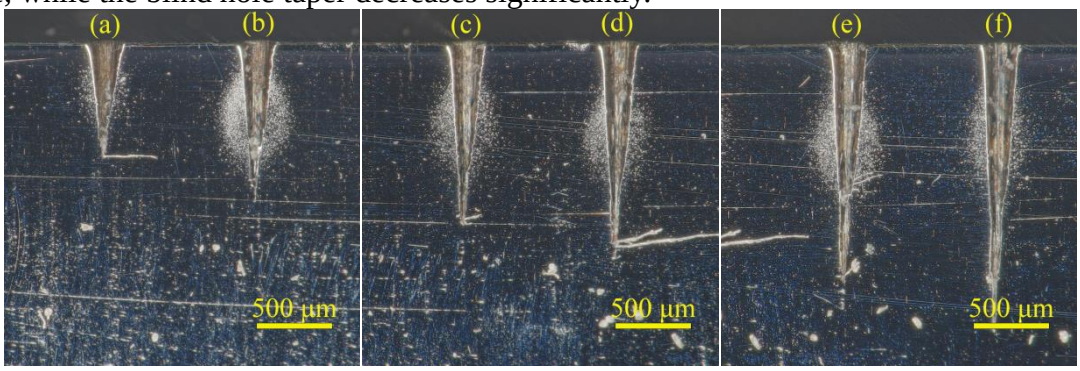

Figure 1: Cross-Sectional View of Blind Hole Processed with Different Single Pulse Energies in Air Environment

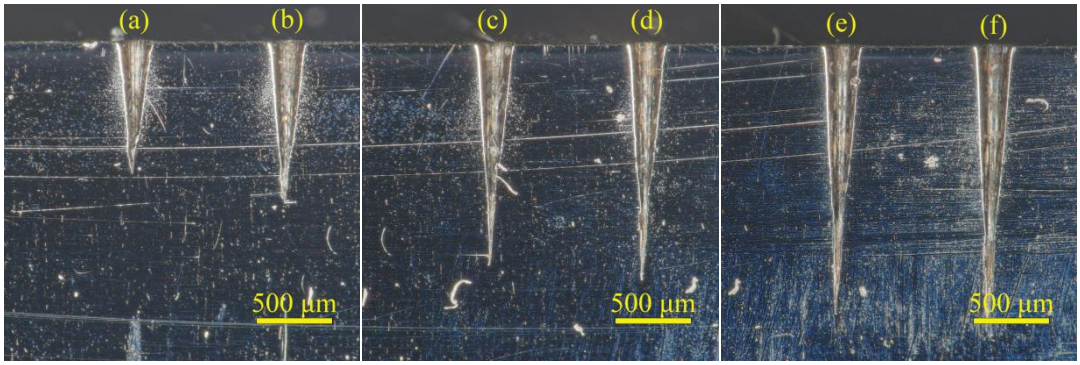

(a)20μJ;(b)40μJ;(c)60μJ;(d)80μJ;(e)100μJ;(f)140μJ

Figure 2: Cross-Sectional View of Blind Hole Processed with Different Single Pulse Energies in Water-Based Environment

From left to right, the single pulse energies are as follows:

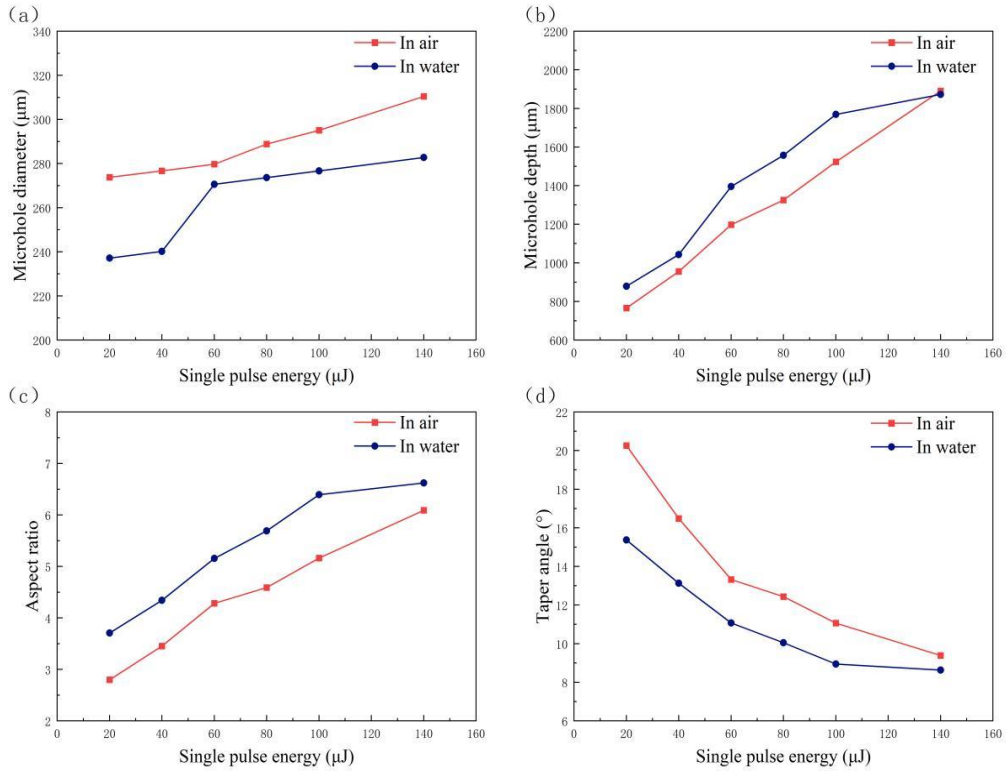

(a)Entrance diameter; (b) Hole depth; (c) Beam Expander Ratio; (d) Taper

Figure 3: Impact of Single Pulse Energy on the Morphology of Blind Holes Processed with Femtosecond Laser in Different Environments

From the analysis of Figure 3(a) and Figure 4, it can be concluded that when the single pulse energy of the laser increases, under the same conditions of other laser parameters, the entrance diameter of the blind hole processed by femtosecond laser shows an increasing trend, regardless of the processing environment. This phenomenon occurs because as the single pulse energy increases, the energy of the laser spot at the entrance of the blind hole also increases, eventually reaching the ablation threshold, which leads to the actual blind hole entrance diameter being larger than the spot diameter[11]. Moreover, when processing high-temperature alloy blind holes directly in the air, the presence of gases such as oxygen in the air acts as an oxidizing agent, which accelerates the femtosecond laser ablation process, resulting in a larger entrance diameter for the blind hole. On the other hand, when processing high-temperature alloy blind holes in a water-based environment, the femtosecond laser must pass through several layers of media—such as the air layer, transparent glass layer, and water layer—before reaching the material surface[12]. Additionally, the cooling effect of the water-based environment causes a partial loss of femtosecond laser energy. Therefore, the entrance diameter of the blind hole processed in the water-based environment is smaller compared to that processed in the air environment.

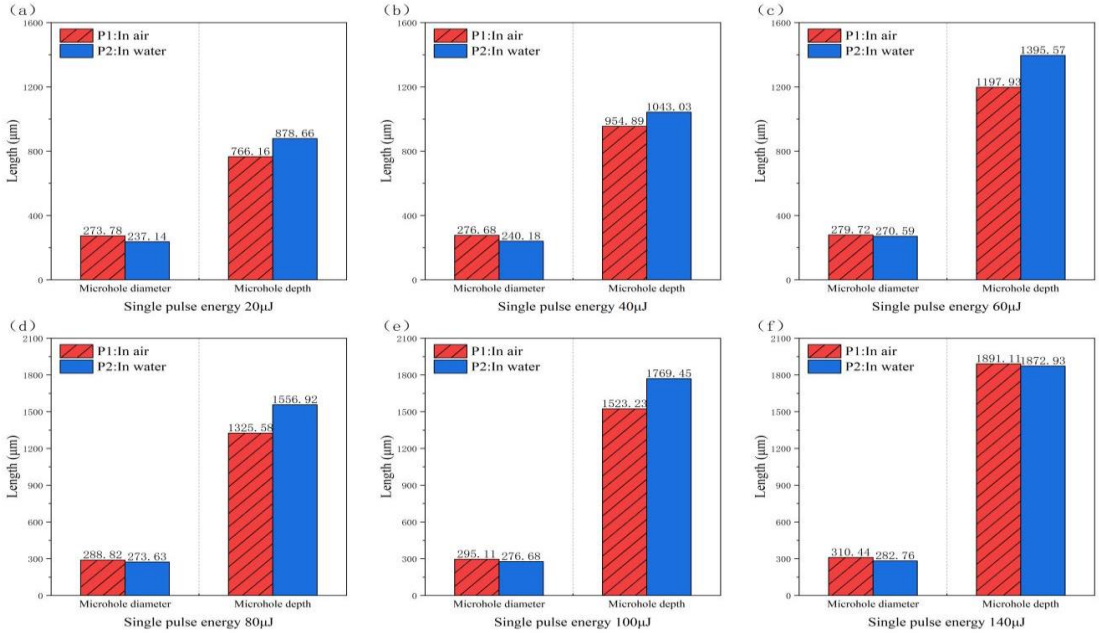

Figure 4: Comparison of Blind Hole Diameter and Depth with Different Single Pulse Energies in Different Processing Environments

From Figure 3(b), it can be seen that in the air environment, the depth of the blind hole increases as the single pulse energy increases. The trend of the blind hole depth change becomes more pronounced, which is due to the fact that at lower pulse energies set in the experiment, the laser energy density is relatively low, resulting in a smaller volume of molten material generated by the laser photons absorbed by the material. This leads to a lower material removal rate. As the single pulse energy increases, the energy density increases, allowing the material to absorb more laser energy, and thus the depth of the blind hole processed by femtosecond laser also increases. In the water-based environment, the depth of the blind hole also increases with the increase in single pulse energy. The change in blind hole depth is more significant than that in the air environment, and the resulting blind hole depth is even greater than that achieved in the air environment. This is because, in a water-based environment, the molten material, plasma, and other residues produced during femtosecond laser drilling are directly absorbed into the water medium, rather than remaining on the hole wall surface. This allows the femtosecond laser to penetrate deeper into the blind hole, resulting in a greater hole depth[13]. Moreover, the extremely high energy density of the femtosecond laser causes the internal temperature of the blind hole to rise sharply. This triggers an evaporation reaction with the water medium, producing high-temperature bubbles. The rapid explosion of these high-temperature bubbles generates high-speed water jets, which impact the micro hole walls, helping to expel the molten residues inside the hole. This enhances the material removal process and increases the depth of the blind hole. As shown in Figure 4, compared to directly processing the blind hole in the air, processing the blind hole in a water-based environment leads to a higher material removal rate. Under the same conditions of femtosecond laser single pulse energy, the blind hole in the water-based environment can achieve greater depth.

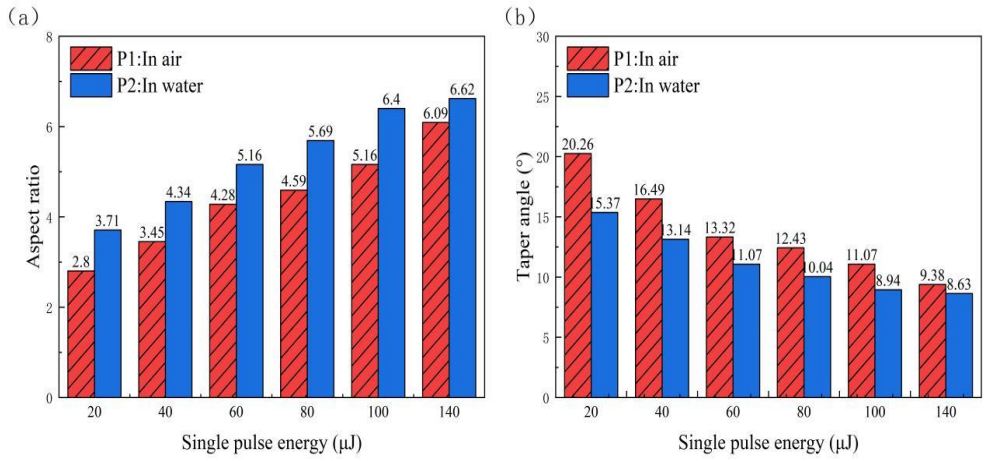

Figure 5: Comparison of Depth-to-Diameter Ratio and Taper of Blind Holes with Different Single Pulse Energies in Different Processing Environments

From the analysis of Figure 5, it can be observed that as the single pulse energy of the laser increases, both the blind hole diameter and depth exhibit a continuous increase. According to Figure 5, as the single pulse energy increases, the depth-to-diameter ratio of the blind hole shows an increasing trend, while the taper decreases. This is because, with the laser spot diameter and the preset maximum hole diameter fixed, the increment in hole diameter becomes smaller as the single pulse energy increases, leading to an increasing ratio of hole depth to diameter. Based on the formulas for the blind hole taper and depth-to-diameter ratio, it can be concluded that the depth-to-diameter ratio of the blind hole is directly proportional to the ratio of hole depth to entrance diameter, while the blind hole taper is inversely proportional to this ratio[14]. Therefore, as the single pulse energy increases, the depth-to-diameter ratio increases, and the taper decreases. From the figure, it can be seen that as the single pulse energy increases, the depth-to-diameter ratio of the blind hole processed in the water-based environment is higher than that of the blind hole processed in the air environment, and the blind hole taper processed in the air environment is significantly smaller.

3.2. Impact of Laser Scanning Speed on the Erosion Hole

Laser scanning speed refers to the movement speed of the laser spot. The speed at which the laser scans directly affects the duration of laser interaction with the material, and the processing time influences the thermal accumulation effect of the laser. This, in turn, has a significant impact on the quality of the laser-processed micro holes[15]. Therefore, selecting an appropriate laser scanning speed is crucial for improving both the efficiency and quality of micro hole processing.

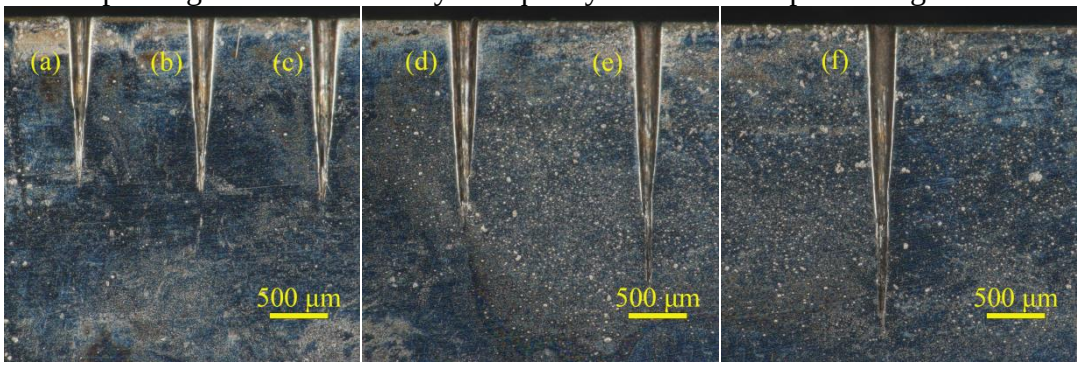

Figure 6: Changing the Laser Scanning Speed for Blind Hole Cross-Sections in Air

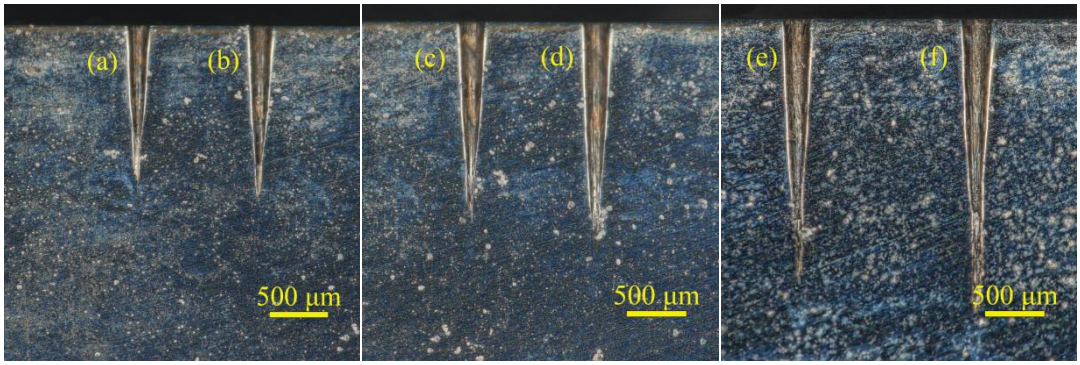

From left to right, the single pulse energies are as follows:(a)800mm/min;(b)600mm/min;(c)400mm/min;(d)200mm/min;(e)100mm/min;(f)50mm/min.

Figure 7: Changing the Laser Scanning Speed for Blind Hole Cross-Sections in a Water-Based Environment

According to the experimental results in Figure 6, Figure 7 and the trend chart in Figure 8, it can be observed that as the femtosecond laser scanning speed increases, in both processing conditions, the entrance diameter, hole depth, and depth-to-diameter ratio of the resulting blind holes show a significant decreasing trend. Meanwhile, the taper angle shows a gradual increasing trend.

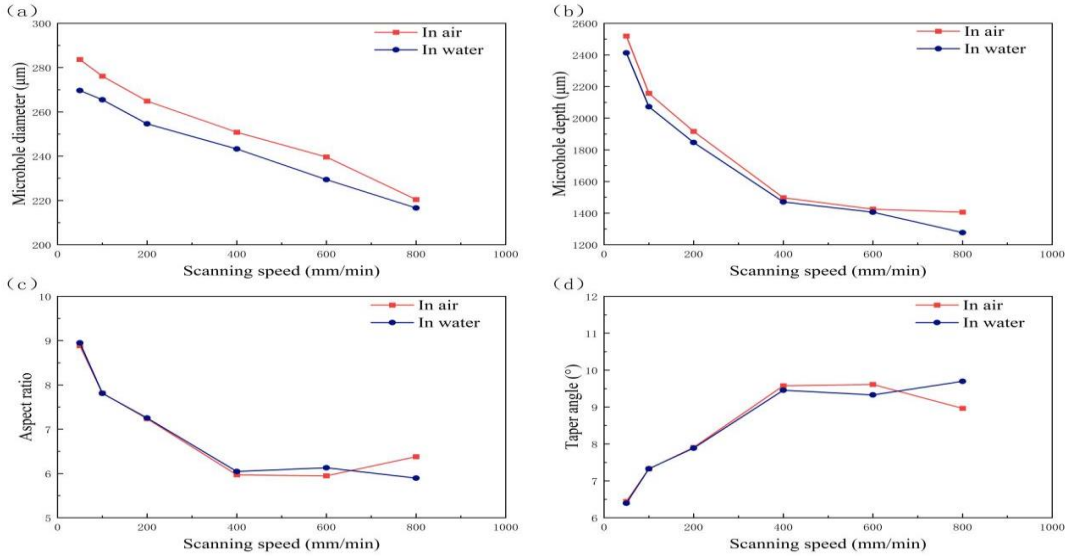

(a) Entrance diameter; (b) Hole depth; (c) Beam Expander Ratio; (d) Taper

Figure 8: Influence of Scanning Speed on the Morphology of Blind Holes Processed by Femtosecond Laser in Different Environments

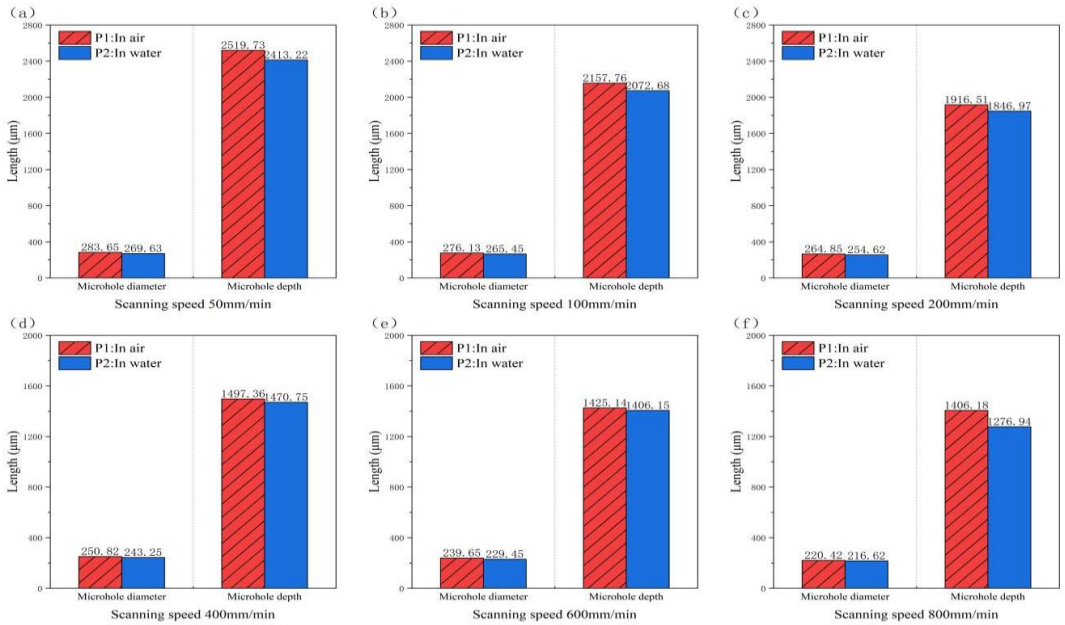

Figure 9: Comparison of Blind Hole Diameter and Depth with Different Laser Scanning Speeds in Different Processing Environments

From Figures 8(a), (b) and Figure 9, it can be seen that the entrance diameter and depth of the blind holes decrease as the laser scanning speed increases. The blind hole entrance diameter and depth from laser processing in air are always larger than those processed in the water-based environment. The fundamental reason for this phenomenon is that, under the same laser parameters, as the laser scanning speed increases, the time for femtosecond laser to act on the high-temperature alloy material decreases, reducing the amount of laser energy the material can absorb, which affects the material removal effect. As the femtosecond laser processes the material in a circumferential cutting manner, the amount of laser energy that can be absorbed by the material deeper in the workpiece decreases, leading to a reduction in the depth of the blind hole. Additionally, due to the Gaussian distribution, the laser spot's interaction time at the entrance of the blind hole also decreases, resulting in a smaller entrance diameter[16]. When the scanning speed is reduced, the interaction time between the laser and the material increases, allowing the high-temperature alloy material to absorb more laser energy, which accumulates as heat and leads to an increase in both the depth and the entrance diameter of the blind hole. Furthermore, in water-assisted laser processing, in addition to the above processes, the laser beam must pass through air and water mediums, and the suspended particles in the water can also interfere with the laser beam[17]. The cooling effect of the water medium reduces the heat-affected zone but also causes a loss of femtosecond laser energy, which is why the blind hole entrance diameter and depth obtained in the water-based environment are smaller than those processed in air.

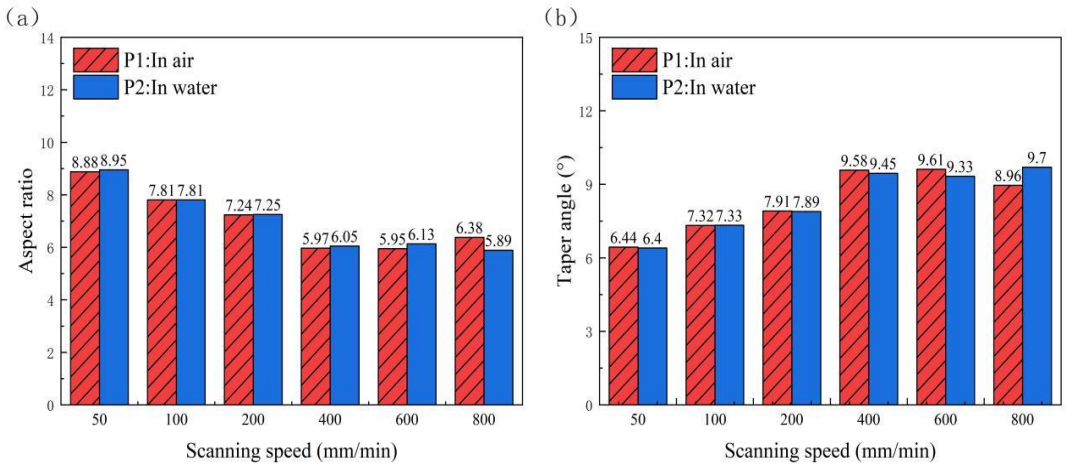

Figure 10: Comparison of Depth-to-Diameter Ratio and Taper of Blind Holes with Different Laser Scanning Speeds in Different Processing Environments

From Figure 10, it can be seen that as the laser scanning speed increases, the depth-to-diameter ratio of the blind holes processed by femtosecond laser decreases, and the taper increases. Additionally, the depth-to-diameter ratio of the blind holes processed in the water-based environment is greater than that of the blind holes processed in the air, and the taper of the blind holes is significantly smaller than that of the blind holes processed in the air. Furthermore, as the laser scanning speed increases, the impact on the blind hole depth and taper in the water-based environment becomes less pronounced. Specifically, when the scanning speed is 800 mm/min, the depth of the blind hole decreases by about 9% compared to the blind hole processed at 600 mm/min, and the taper increases by 4%. When the scanning speed is reduced to 400 mm/min, the depth decreases by about 20% compared to the blind hole processed at 200 mm/min, while the taper increases by nearly 19%. Therefore, it can be concluded that when processing high-temperature alloy blind holes with femtosecond lasers in a water-based environment, a lower laser scanning speed should be selected to ensure a smaller hole taper while maintaining laser processing efficiency.

4. Conclusions

Based on the analysis of the influence trends of various factors on the blind hole quality indicators (such as blind hole size, taper, and depth-to-diameter ratio) and the experimental processing conditions, it can be concluded that the single pulse energy has a stronger impact on the hole quality of femtosecond laser processing of high-temperature alloy blind holes compared to the laser scanning speed. In the analysis of blind hole entrance diameter and taper, single pulse energy is the most influential factor, while scanning speed has a negligible impact on the quality indicators of the blind hole. Additionally, from the above analysis, it can be deduced that laser scanning speed also affects the drilling efficiency. In practical production, drilling efficiency is one of the essential criteria for evaluating micro hole processing technology[18]. Therefore, selecting an appropriate laser scanning speed can ensure the quality of micro hole processing while meeting laser processing efficiency requirements.

According to the micro hole quality characterization requirements, the taper of a micro hole is more important than the entrance diameter in evaluating the quality of the micro hole. Considering the experimental processing conditions and the quality of the blind hole inner wall, the optimal processing parameters for this experiment are as follows:

For single pulse energy in the range of 10μJ to 140μJ, the optimal processing parameters are:

water-based assistance, single pulse energy of 100μJ, scanning speed of 400mm/min, pulse width of 276fs, and repetition frequency of 50kHz.

For laser scanning speeds in the range of 50mm/min to 800mm/min, the optimal processing parameters are: water-based assistance, scanning speed of 50mm/min, single pulse energy of 140μJ, pulse width of 276fs, and repetition frequency of 50kHz.

Acknowledgements

1) National Natural Science Foundation of China (52375434)

2) Major Project of Basic Science (Natural Science) Research in Colleges and Universities in Jiangsu Province (23KJA460003)

3) Teaching Reform Project of Degree and Postgraduate Education in Jiangsu Province (JGKT24_C084)

References

[1] Wang Bo, Yin Shaohai. Application of thermal barrier coating technology on turbine blades of aero engines [J]. China New Technology and New Products, 2018(08): 18-19.

[2] Zhang Zhiqiang, Song Wenxing, Lu Haiying. Research on the application of thermal barrier coatings on turbine blades of aero engines [J]. Aero Engine, 2011, 37(02): 38-42.

[3] Gao Ji, Cao Guoqiang. Special processing technology for micro-hole and its development status [J]. Mechanical Design and Manufacturing, 2005(07): 169-171.

[4] Lv Da, Han Yangguang, Cui Yi, et al. Thermal processing technology of GH4169 high-temperature alloy [J]. Metal Heat Treatment, 2023, 48(08): 132-137.

[5] Wang Huiyang, An Yunqi, Li Chengyu, et al. Research progress of nickel-based high-temperature alloy materials [J]. Materials Review, 2011, 25(S2): 482-486.

[6] Song Yan, Wang Peng, Yang Zhigang, et al. Research on the quantitative statistical distribution characterization method of niobium-rich phase in GH4169 alloy and its application [J]. Metallurgical Analysis, 2024, 44(04): 1-8.

[7] Kang Xinlong. Principle and application of electrical discharge composite machining [J]. Mechatronic Product Development and Innovation, 2007, 04: 175-176.

[8] Yin Dapeng. Cooling film hole machining technology for aero-engine turbine blades [D]. Dalian University of Technology, 2014.

[9] Hu Chunyan, Liu Xinling, Tao Chunhu, et al. Study on the damage behavior of DD6 single crystal high-temperature alloy film holes processed by electrohydraulic machining [J]. Rare Metal Materials and Engineering, 2019, 48(10): 3190-3194.

[10] Fan Runze, Xie Herui, Xu Jingji, et al. Research progress on laser processing of gas film hole remelting layers [J]. Casting Technology, 2023, 44(09): 779-795.

[11] Prithpal S, Pramanik A, Basak A K, et al. Developments of non-conventional drilling methods-a review [J]. The International Journal of Advanced Manufacturing Technology, 2020, 106: 2133-2166.

[12] Liu Xinling, Tao Chunhu, Liu Chunjiang, et al. Evolution analysis of film hole machining methods for aero-engine blades [J]. Materials Review, 2013, 27(21): 117-120.

[13] Zhang Xiaobing, et al. Laser processing of small holes technology [M]. Beijing: National Defense Industry Press, 2020. 9.

[14] Tao S, Wu B, Lei S. Study of laser beam propagation in microholes and the effect on femtosecond laser micromachining [J]. Journal of Applied Physics, 2011, 109(12): 1.

[15] Povarnitsyn M E, Fokin V B, Levashov P R. Microscopic and macroscopic modeling of femtosecond laser ablation of metal [J]. Applied Surface Science, 2015.

[16] Du Juan. Molecular dynamics simulation of femtosecond laser processing of silicon [D]. Harbin Institute of Technology, 2012.

[17] Chen Bing, Zhu Weihua, Chen Peng, et al. Molecular dynamics simulation of femtosecond laser ablation mechanism of CuZr amorphous alloy [J]. Laser & Optoelectronics Progress, 2015, 52(4): 129-133.

[18] Ma Guoqing, Xiao Qiang. Overview of femtosecond laser micropore processing [J]. Laser & Infrared, 2020, 50(06): 651-657.